

Oliver A. Meissner
Claus-Georg Schmedt
Kathrin Hunger
Holger Hetterich
Ronald Sroka
Johannes Rieber
Gregor Babaryka
Bernd Manfred Steckmeier
Maximilian Reiser
Uwe Siebert
Ullrich Mueller-Lisse

Endovascular optical coherence tomography ex vivo: venous wall anatomy and tissue alterations after endovenous therapy

Received: 15 May 2006
Revised: 12 November 2006
Accepted: 11 January 2007
Published online: 8 February 2007
© Springer-Verlag 2007

O.A. Meissner and C.-G. Schmedt
contributed equally to this work.

O. A. Meissner (✉) · K. Hunger ·
M. Reiser · U. Mueller-Lisse
Institute for Clinical Radiology,
Ludwig Maximilians University,
Ziemssenstr. 1,
80336 Munich, Germany
e-mail: oliver.meissner@med.uni-
muenchen.de
Tel.: +49-89-51609125
Fax: +49-89-51609112

C.-G. Schmedt · B. M. Steckmeier
Department of Vascular Surgery
and Phlebology,
Ludwig Maximilians University,
Ziemssenstr. 1,
80336 Munich, Germany

H. Hetterich · J. Rieber
Division of Cardiology,
Ludwig Maximilians University,
Ziemssenstr. 1,
80336 Munich, Germany

R. Sroka
Laser Research Laboratory,
LIFE-Center,
Ludwig Maximilians University,
Ziemssenstr. 1,
80336 Munich, Germany

G. Babaryka
Institute of Pathology,
Ludwig Maximilians University,
Ziemssenstr. 1,
80336 Munich, Germany

U. Siebert
Institute for Technology Assessment and
Department of Radiology,
Massachusetts General Hospital,
Harvard Medical School,
Boston, MA, USA

U. Siebert
Department of Public Health,
Medical Decision Making and
Health Technology Assessment,
University for Health Sciences,
Medical Informatics and Technology,
Hall/Innsbruck, Austria

O. A. Meissner
Siemens AG Medical Solutions,
Forchheim, Germany

Abstract Endovascular optical coherence tomography (OCT) is a new imaging modality providing histology-like information of the venous wall. Radiofrequency ablation (RFA) and laser therapy (ELT) are accepted alternatives to surgery. This study evaluated OCT for qualitative assessment of venous wall anatomy and tissue alterations after RFA and ELT in bovine venous specimens. One hundred and thirty-four venous segments were obtained from ten ex-vivo bovine hind limbs. OCT signal

characteristics for different wall layers were assessed in 180/216 (83%) quadrants from 54 normal venous cross-sections. Kappa statistics (κ) were used to calculate intra- and inter-observer agreement. Qualitative changes after RFA (VNUS-Closure) and ELT (diode laser 980 nm, energy densities 15 Joules (J)/cm, 25 J/cm, 35 J/cm) were described in 80 venous cross-sections. Normal veins were characterized by a three-layered appearance. After RFA, loss of three-layered appearance and wall thickening at OCT corresponded with circular destruction of tissue structures at histology. Wall defects after ELT ranged from non-transmural punctiform damage to complete perforation, depending on the energy density applied. Intra- and inter-observer agreement for reading OCT images was very high (0.90 and 0.88, respectively). OCT allows for reproducible evaluation of normal venous wall and alterations after endovenous therapy. OCT could prove to be valuable for optimizing endovenous therapy in vivo.

Keywords Optical coherence tomography · Endovenous laser therapy · Endovenous radio-frequency therapy

Introduction

Endovascular optical coherence tomography (OCT) is a new imaging technique based on the use of infrared light, permitting visualization of the vascular wall and lumen with a resolution of 15–20 μm [1–3]. This is ten- to 20-times higher than that offered by any of the currently available imaging methods. The first *ex vivo* clinical studies of coronary and below-the-knee arteries have shown that OCT is not only capable of distinguishing the mural layers constituting normal vessel architecture but also identifies individual components of atherosclerotic plaques [4–8]. To date, however, the value of OCT in imaging the venous vasculature has not been systematically studied.

Endovenous thermal therapy of incompetent veins is a promising alternative to surgical ligation and stripping [9–11]. The two most commonly used minimally invasive techniques are radiofrequency ablation (RFA) or endovenous laser therapy (ELT). The underlying principle of RFA is direct heating of the venous wall by high-frequency electromagnetic waves applied via a special probe with bipolar electrodes [12]. The principle of ELT is photon absorption in blood and venous wall tissue with consecutive heating [13, 14].

First series and controlled trials reported on high clinical efficacy of endovenous therapy with low complication rates [15–19]. The consequences of endovenous treatment, such as venous wall thickening, a reduction in luminal diameter, thrombus formation or obliteration are currently assessed either clinically, based on duplex ultrasound findings, or on phlebography [17, 20]. The methods in routine clinical use are not capable of differentiating between the different layers of the venous wall. Moreover, effects of endoluminal therapy cannot be visualized directly during the procedure.

The objective of our study was to investigate the capacity of OCT to characterize the structure of the normal venous wall and to distinguish it from alterations after endovenous thermotherapy. Differentiation of the type of change in the venous wall following RFA or ELT at different energy levels can directly influence clinical and therapeutic management. The experimental method was based on a standardized bovine hind limb model, with both untreated, normal venous segments and segments that had been exposed to the effects of RFA or ELT. Findings were compared with the results of histopathology as the reference standard.

Materials and methods

Specimens

All examinations were performed using a standardized bovine hind limb model that has been routinely used in

vascular surgery for venous studies [21]. A total of ten amputated hind limbs were obtained from ten freshly slaughtered cows (age: 18–24 months, weight: 550–650 kg; left hind leg). Following *in situ* exposure of the subcutaneous veins (third common digital vein and the lateral saphenous vein), the veins were supplied proximally and distally with 6 F or 5 F ports, respectively, which were fixed in place by suture. Subsequently, side branches were ligated. Special care was taken not to open the veins, in order to prevent damage to the venous wall. The prepared bovine limbs were then attached by tubes to an infusion system in order to maintain a perfusion pressure of 3–5 kPa in the venous lumen. Prior to the OCT examination, the venous specimens were carefully irrigated with a 0.9% normal saline solution to remove adherent blood clots. The diameter of the veins to be examined averaged 3.5 mm. Lengths of the vessel segments examined was 15 cm. In order to exactly match the OCT images with the corresponding histological sections, suture material (Ethicon Ethibond Excel; Johnson & Johnson Intl.) was fixed to perivascular tissue at certain points. Moreover, the position of the OCT catheter could be visualized through the venous specimens because of the rotating infrared light signal at the catheter tip. Time between amputation and OCT imaging did not exceed 3 h. The experimental protocol was approved by our Institutional Review Board.

Principles of OCT

The OCT used in this study was an intravascular system manufactured by LightLab Imaging (System M1; LightLab Imaging, Westford, Mass.). Based on the principles of interferometry [22–24], OCT uses a broad-spectrum light source (superluminescence diode, SLED) that, in the near-infrared band, emits a wavelength of $1,300 \pm 20$ nm. This low-coherency light source permits spatial axial resolution in the range of 15–20 μm in non-transparent tissue. For subsequent interferometric analysis, the light coming from the light source is entered into a beam splitter and divided into two arms: the sample arm and the reference arm. The sample arm of the light is introduced into the vessel through a thin glass fiber measuring 60 μm in diameter that is contained within a highly flexible silicone sheath about 0.4 mm in diameter. At the tip of the fiber, a prism refracts the light radially toward the venous wall. Light reflected by adjacent structures, such as the internal or external elastic membrane, is transmitted back along the same path to the optical unit (Michelson interferometer), where image reconstruction takes place. The reference arm of the light is reflected by a rotating reference mirror and passes back into the optical interferometer through the same fiber. For optical coherence measurements, the signal from the sample arm is superimposed on the signal from the reference arm. Interference can only be measured when differences in length between both arms are smaller than

the coherence length of the light. Therefore, depth resolution is based on the adjustable length of the reference path length in the interferometer. To achieve different penetration depths in tissue, the reference mirror has multiple steps on its surface, whose position is altered by fast rotation (3,000 cycles/min). By variation of the reference path length, a depth scan, analogous to the A-scan in ultrasound imaging, is generated. Secondary to scattering and absorption in the tissue, penetration depth in the vascular wall is limited to 1.5–2 mm. Rotation of the glass fiber within the silicone sheath yields a tomographic cross-sectional image. In addition, the option of automated catheter pull-back makes it possible to scan a vascular segment of up to 50 mm in length during one examination. In the current study, we worked with an image acquisition rate of 5 Hz and a pull-back velocity of 1.0 mm/s. The acquired OCT data were saved as digital film sequences (.avi) or individual frames (.tiff) and quantified offline using a commercially available software (Tape Measure Indec Systems, Mountain View, Calif.).

Endovenous thermal therapy

The clinical principles of the RFA procedure and ELT have been previously described in detail [25, 26]. The radio-frequency probe with its retractable bipolar electrodes was introduced via a sheath system. After positioning the tip of the probe and of the electrodes, respectively, the RFA catheter was activated and the energy directly applied into the venous wall up to a set point temperature of 85°C, which was maintained by a feed-back mechanism. The probe was manually withdrawn at a speed of approximately 3.0 cm/min (0.5 mm/s) [27]. Average diameter of the veins to be examined was 1.5–3.5 mm. Average length of the venous specimens was 150 mm.

With ELT, monochromatic light is introduced through a fiber optic line into the venous lumen and the venous wall is heated by absorption of photons [18, 28]. There are several different treatment procedures using different laser wavelengths, energy levels and withdrawal protocols; hence, the therapy is not standardized [13, 29, 30]. In our experimental setting, ELT was performed using a diode laser (CERALAS D15 ELVeS; CeramOptec, Bonn, Germany) emitting light with a wavelength of 980 nm, which is transported via a 600- μ m bare-tipped optical fiber. The laser energy was applied by interval illumination using 3, 5, and 7 Watts (W), respectively. Laser pulse duration was 1.5 s, and one pulse was applied after incremental repositioning of the laser waveguide every 3 mm. This resulted in energy densities of 15 Joules (J), 25 J or 35 J per cm, respectively. As with RFA, average lengths of each vein segment treated was 150 mm.

In order to simulate clinical setting and for ELT to produce their maximum thermal effects, the presence of blood is required. For this reason, all treated veins were

perfused with heparinized bovine blood prior to thermal therapy.

After treatment, application devices and treated veins were examined macroscopically with standardized in-situ and ex-situ preparation and documentation. Before OCT examination veins were again washed with saline solution in order to remove residual blood clots.

Histology

All histological specimens were fixed in formalin for 24 h. After paraffin embedding, the material was sliced at marked imaging sites using a microtome at a slice-thickness of 4 μ m. All blocks were stained with hematoxylin and eosin and counterstained with Elastica-van Gieson (EvG) for better delineation of fibrous tissue. All venous cross-sectional segments were evaluated by light microscopic examination. Histological sections were then saved digitally at different magnifications (40 \times and 100 \times).

Comparison between OCT images and histology

Fifteen histological cross-sections were obtained from each hind limb for a total of 150 histological cross-sections. Sixteen out of 150 (11%) of the histological cross-sections could not be interpreted due to damage to the venous wall secondary to preparation, staining and fixation. The remaining 134 venous cross-sections were correlated with corresponding postinterventional OCT images. In order to more precisely estimate distinction of different wall layers, as well as the effects of RFA and ELT, OCT images were displayed as quarters (i.e., right and left upper and lower quarters, respectively) of the original OCT image.

At first, a consensus was established by a pathologist (G.B.), a vascular surgeon (C.G.S.) and a radiologist (O.M.) regarding the anatomical correlation between the OCT images and the corresponding venous segments. In addition to external marking, structures such as vascular side branches or venous valves were used for orientation. Each venous segment received a unique number code.

For image interpretation, the magnification mode of the OCT system was used. This function visualizes OCT images at full spatial resolution of 10 \times 5 μ m per pixel in the axial plane.

The OCT images of untreated venous segments were evaluated for delineation of the different wall layers. We distinguished between the tunica intima (I), the tunica media (M), the tunica adventitia (A) and the internal and external elastic membrane.

In the OCT images of the venous segments treated with RFA and ELT, attention was paid to the type of changes that could be observed in each individual mural layer. The number of positive delineations was recorded for each of the criteria and each observer. Number and percentage of

images with agreement between observers were also recorded.

OCT image analysis and histological evaluation were each performed by two independent evaluators (K.H., H.H. and G.B., J.R., respectively), blinded to the results of the corresponding study. K.H. is a radiologist in training with more than 2 years' experience in OCT readings. H.H. is a cardiologist in training with the same level of experience in OCT evaluation.

In cases where the examiners reached divergent conclusions, a consensus reading was established by requiring both examiners to reach a joint conclusion. To determine intraobserver variability, the OCT data set was evaluated twice by one evaluator (K.H.).

Statistics

Dichotomous variables were expressed as proportions with exact 95% confidence intervals (95% CI) and continuous variables as mean±SD. OCT inter- and intra-observer agreement were assessed using the kappa (κ) statistic with the κ -test of concordance [31]. The statistical design and data analysis of this study was planned in advance and

performed by a licensed biostatistician (U.S.). Statistical analyses were performed using SPSS v. 12.0 (SPSS, Chicago, Ill.).

Results

OCT of untreated venous segments

A total of 180/216 (83%) quadrants from 54 normal vessel segments were available for comparison. In 12/216 (6%) quadrants artifacts secondary to histological fixation resulted in inability to evaluate the corresponding segment, while, in 24/216 (11%) quadrants a complete eccentric position of the probe resulted in OCT images being either over- or under-illuminated.

OCT images of untreated normal vessel segments revealed a characteristic three-layered appearance. While OCT clearly distinguished tunica media and tunica adventitia layers as defined by histology, it was more difficult to discern tunica intima, inner elastic membrane, and transition between tunica media and tunica adventitia. The external elastic membrane was not visualized by OCT (Fig. 1). Tables 1 and 2 summarize qualitative OCT image

Fig. 1a–d Histological (hematoxylin/eosin staining; magnification 40 \times) and OCT images of a normal venous segment. **a** Histology shows a three-layered appearance of the vessel wall with clear differentiation of the tunica intima (*I*), tunica media (*M*) and tunica adventitia. The vertical lines represent fixation artifacts (asterisks). **b** In the corresponding OCT image there is a signal-rich appearance of the tunica intima (*I*), while the tunica media (*M*) is predominantly low in signal, but traversed by several high-signal collagenous and elastic fibers. The tunica adventitia (*A*) appears high in signal. **c, d** Zoomed-in views of **a** and **b** for better delineation of *I*, *M* and *A* (white lines indicating transition between *I/M* and *M/A*, respectively). *C* artifact caused by the OCT catheter, *L* lumen. Bar=1 mm

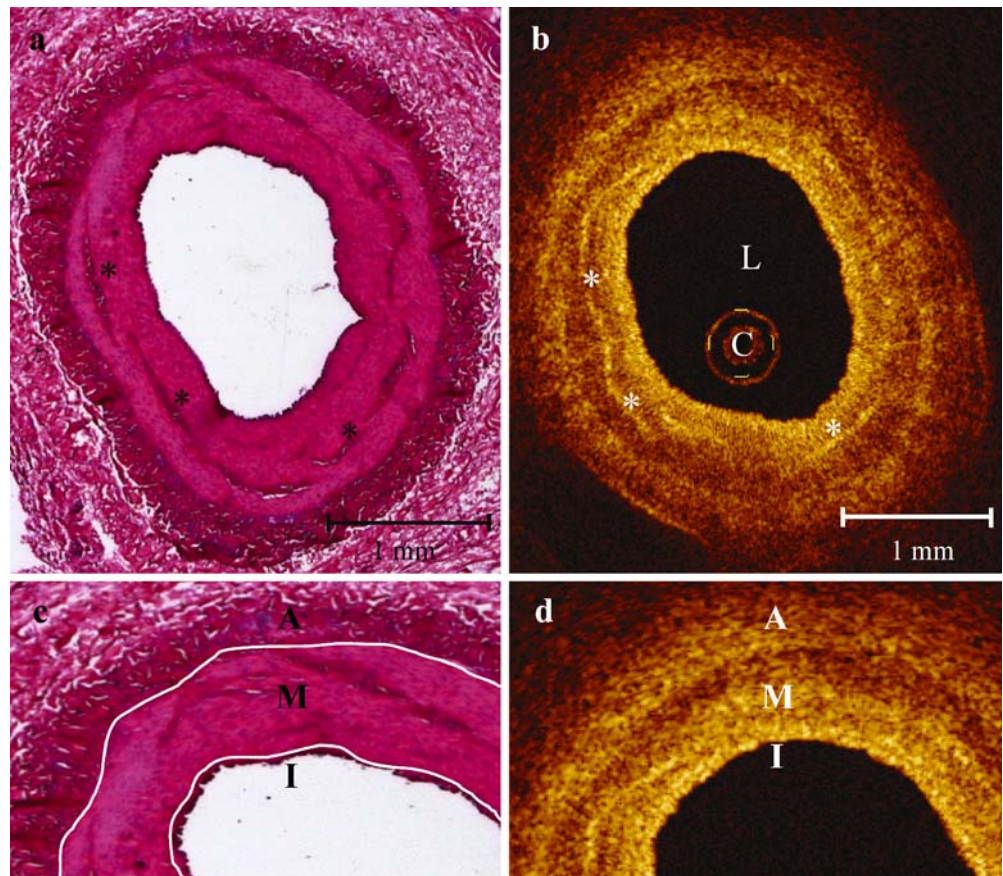


Table 1 Differentiation of vessel wall layers in untreated venous segments ex vivo based on OCT signal characteristics: comparison of a consensus reading of OCT (*cOCT*) and histology (*cHisto*) in $n=180/216$ quadrants (95% CI 95% confidence interval)

| Vessel wall components | cOCT | cHisto | Agreement | 95%CI |
|-----------------------------|------|--------|------------|---------|
| Tunica intima | 127 | 180 | 127 (71%) | 63–77% |
| Membrana elastica interna | 127 | 180 | 127 (71%) | 63–77% |
| Tunica media | 180 | 180 | 180 (100%) | 98–100% |
| Transition media/adventitia | 154 | 180 | 154 (86%) | 80–90% |
| Tunica adventitia | 179 | 180 | 179 (99%) | 97–100% |

criteria of the normal venous wall and agreement between the consensus of OCT image criteria and the consensus of histologic diagnosis.

The intra-observer and inter-observer agreement for characterization of different venous wall layers by OCT signal criteria was very good (κ values of 90% and 88%, respectively; $P<0.001$).

OCT of venous segments after thermal treatment

OCT images of the 13 venous segments treated with RFA showed increase in vessel wall thickness and loss of distinction between vessel wall layers (Table 3, Fig. 2). Standardized in-situ preparations showed no macroscopic evidence of punctuate lesions, but marked circumscribed indurations of the vessel wall and contraction of the vessel lumen. Histological slices revealed extensive circular swelling of the entire vascular wall, with loss of definition of vascular contours. The endothelial cells appeared mostly disintegrated.

Of 67 venous segments treated with ELT, 22 segments were exposed to an energy density of 15 J/cm, while in 23 vessel segments an energy density of 25 J/cm and in 22 an energy density of 35 J/cm was used. Postinterventional OCT and corresponding histological cross sections after

ELT demonstrated different degrees of thermal damage to the vessel wall, varying according to the laser energy density used (Table 3, Figs. 3, 4, 5).

Discussion

Our results demonstrate that the three-layered structure of the venous wall, consisting of tunica intima, tunica media and tunica adventitia, can be clearly visualized on the basis of OCT signal characteristics. The different mural layers exhibited the same OCT signal criteria as had been identified in the first ex vivo studies of coronary and peripheral arteries [4, 32]. As with healthy arterial specimens, due to the resolution of OCT, the tunica intima of the normal venous wall could only be distinguished from the similarly high-signal internal elastic membrane when its thickness exceeded 15 μm . Unlike in muscular-type arteries, the tunica media of the venous wall (whose signal at OCT is low) includes a large proportion of elastic fibers. OCT visualized these interspersed bundles of elastic fibers as inhomogeneous layers of high signal intensity. Nonetheless, differentiation between tunica media and tunica adventitia was possible by means of OCT in 179 of 180 venous cross sections. This implies that interposition of elastic fibers does not significantly limit differentiation of

Table 2 Differentiation of vessel wall layers in untreated venous segments ex vivo based on OCT signal characteristics: description of histological findings and OCT signal characteristics of the different mural layers of the normal venous wall

| Normal venous wall | Histology | OCT |
|---------------------------|---|--|
| Tunica intima | Single or multiple layers of endothelial cells | Infrequently distinguishable from the internal elastic membrane, with high signal intensity, between 4–50 μm in thickness |
| Internal elastic membrane | Irregularly configured layer of collagenous fiber | High signal intensity, transition between the tunica intima and media |
| Tunica media | Concentric layers of smooth muscle fibers, collagen bundles and elastic fibers | Predominantly low-signal intensity, with interspersed bright signals representing collagen bundles and elastic fibers |
| External elastic membrane | Not identifiable | Not identifiable |
| Tunica adventitia | Concentrically ordered collagen and elastic fibers, with small blood vessels (vasa vasorum) | Inhomogeneous, predominantly high-signal, depending on amount of collagen a/o elastic fibers |

Table 3 Qualitative description of histological findings and OCT signal characteristics after RFA and ELT at different energy levels on the mural layers of bovine hind limb veins ex vivo (*I* tunica intima, *M* tunica media, *A* tunica adventitia, *IEM* internal elastic membrane)

| | Histology | OCT |
|---|--|--|
| RFA | Extensive circular swelling of entire vascular wall, loss of vascular contours, endothelial cells appear disintegrated | Increase in vessel wall thickness, homogeneously high signal intensity of all different vessel wall layers (Fig. 2) |
| ELT Low energy density (15 J/cm) | Localized tissue defect affecting I and IEM, no transmural defect | band-like high-signal intensity in the defect crater, representing I and IEM in areas of tissue carbonization (Fig. 3) |
| ELT Intermediate energy density (25 J/cm) | Localized tissue ablation affecting I, M, A | High-signal intensity defect, representing I, M, A in areas of tissue carbonization (Fig. 4) |
| ELT High energy density (35 J/cm) | Focal transmural vessel wall disruption with disintegration of vessel wall layers | Focal transmural vessel wall defect with carbonization of perivascular tissue (Fig. 5) |

venous wall layers by OCT. The high degree of reproducibility of the recorded OCT signal characteristics agrees to a great extent with data derived from atherosclerotic arterial segments. For example, the method was able to distinguish with high sensitivity and specificity between predominantly fibrotic, predominantly lipid-rich and predominantly calcified atherosclerotic plaques [7, 33]. The reported inter-observer and intra-observer agreement (κ scores of 0.88 and 0.91, respectively), correspond closely to data returned in this study.

Because of its unique detail resolution of 15–20 μm , OCT is the only currently available imaging method that can visualize the different layers of the normal venous wall. The spatial resolution of this method is ten- to 20-times higher than, for example, intravascular ultrasound (IVUS), which has been considered the ‘gold standard’ for imaging of the vascular wall. Newer methods such as CT- or MR-plebography permit visualization of the contours of the vascular lumen but allow only limited visualization of the venous wall. Because of high tissue contrast, MRI certainly

has the potential for imaging the vascular wall. With a spatial resolution currently limited to a maximum of 400 μm , however, it is clearly inferior to OCT.

In addition to visualization of the normal venous wall, the present study has shown for the first time that the effects of different endoluminal thermal therapy methods in the venous wall can be reliably assessed with OCT. Following RFA treatment, there was in all segments a homogenization of signal intensity throughout the venous wall, with disappearance of boundaries between the tunica intima, tunica media and tunica adventitia. However, at power settings between 0 and 6 W, no penetrating wall damage was observed in our study. A possible explanation could be the homogeneous, circular distribution of thermal energy to the vessel wall, with the help of electrodes of the radiofrequency probes and the temperature feedback mechanism that automatically ensures homogeneous application of energy.

Effects of ELT treatment on the venous wall differed from those of RFA application. Depending on the laser

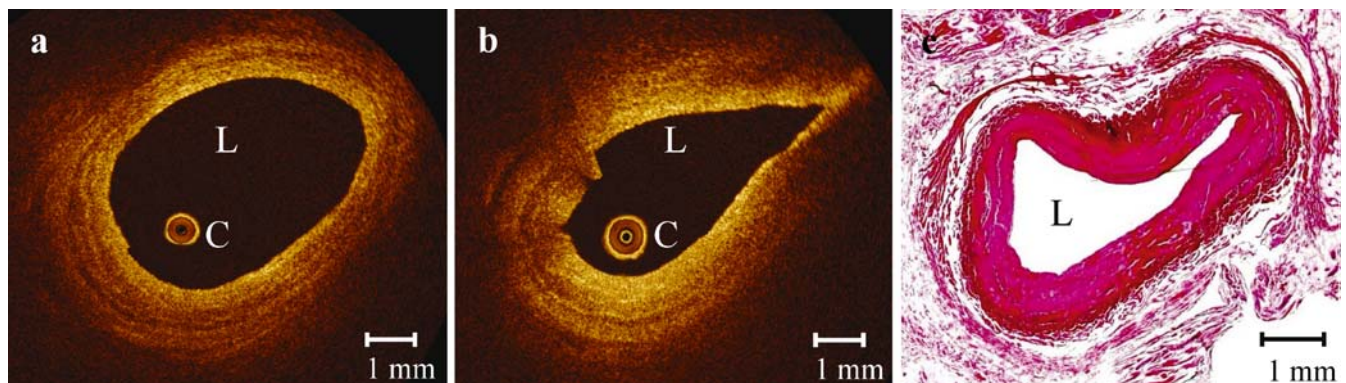


Fig. 2a–c Subcutaneous bovine leg vein before and after RFA. **a** OCT image before RFA treatment reveals normal three-layered appearance of the vessel wall with normal lumen width. **b** OCT image immediately after RFA treatment shows homogenization of signal intensity with loss of the normal wall structure and

significant lumen loss. **c** Histological cross section (hematoxylin/eosin staining; magnification 40 \times) with a circular swelling of the entire vascular wall, reduced clarity of vascular contours and significant increase in the thickness of the vascular wall. *C* artifact caused by the OCT catheter, *L* lumen. *Bar*=1 mm

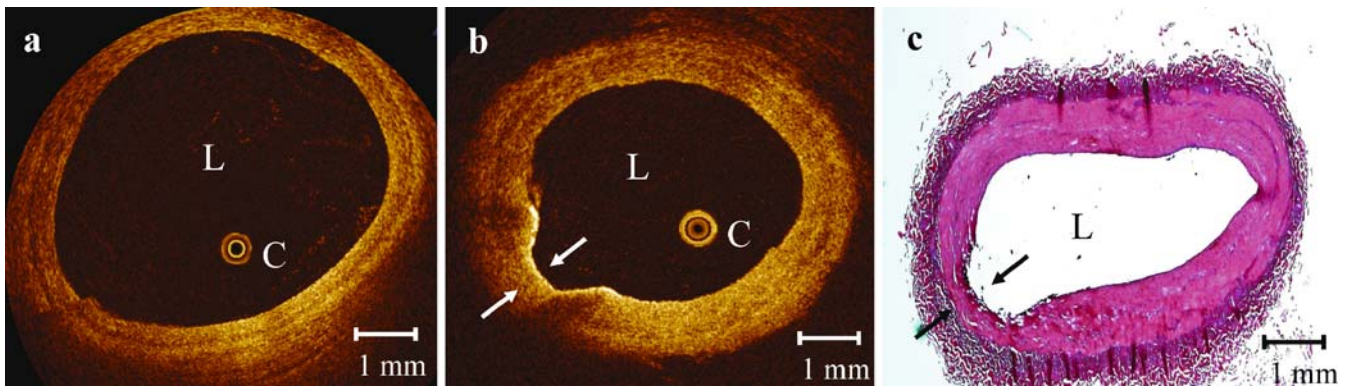


Fig. 3a–c Subcutaneous bovine leg vein before and after ELT with low energy density (15 J/cm). **a** OCT image before ELT reveals normal three-layered appearance of the vessel wall with normal lumen width. **b** OCT image immediately after ELT treatment demonstrates localized tissue ablation with a depressed, but not transmural wall defect and band-like high-signal intensity in the

defect crater, representing carbonization of the tunica intima (white arrows). No significant thermal changes are seen on the opposite site. **c** Histological cross section (hematoxylin/eosin staining; magnification 40 \times) shows the depressed defect with marginal coagulation and carbonization of the tunica intima (black arrows). *C* artifact caused by the OCT catheter, *L* lumen

energy applied, effects of ELT ranged from isolated coagulation of the tunica intima at low energy levels (15 J/cm), to transmural coagulation at intermediate energy levels (25 J/cm) and complete, punctuate vessel wall perforation with destruction of the perivascular adipose tissue at high energy levels (35 J/cm). Such changes of the venous wall in relation to the applied laser energy density have also been reported by other authors in their examinations [27, 34]. Moreover, Proebstle et al. [14] found that ELT results in significant heating of the fiber tip to temperatures in excess of 1,000 $^{\circ}$ C. It has to be assumed that this is caused by the absorption of laser light in carbonized tissue accumulating at the fiber tip. Therefore, the thermal effect takes place not only by absorption of the laser light by hemoglobin or vessel wall structures, but also

by convection of heat energy from the fiber tip to the surrounding tissue, consequently leading to complete destruction of the wall on one side, whereas parts of the vessel wall on the opposite side show no, or only minor, thermal changes. In cases of incomplete circumferential denaturation of the vessel wall, however, regeneration and recanalization is theoretically possible. This has been clinically observed with an incidence of 10–23% [30, 35]. On the one hand, our preliminary ex-vivo series indicates that the application of ELT perhaps should be modified in order to ensure homogenous, circumferential thermal denaturation of the vessel wall, while avoiding perforation of the venous wall segments and possible, subsequent damage to perivascular structures. On the other hand, our results imply that OCT could be used to detect and localize

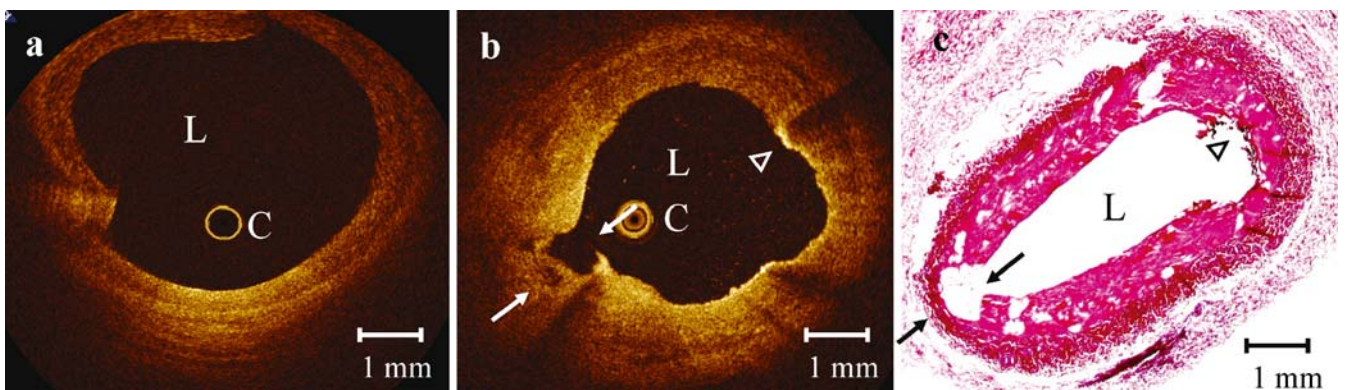


Fig. 4a–c Subcutaneous bovine leg vein before and after endoluminal Laser treatment (ELT) with intermediate energy density (25 J/cm). **a** OCT image before ELT reveals normal three-layered appearance of the vessel wall with normal lumen width. **b** OCT image immediately after ELT treatment demonstrates local ablation of tunica intima, tunica media and tunica adventitia (white arrows) in areas of tissue carbonization. Additional high-signal intensity

opposite to the treated area implies that during passage the active tip of the laser probe touched the venous wall opposite to the intended place of treatment (white arrowhead). **c** Histological cross section (hematoxylin/eosin staining; magnification 40 \times) with ablation of all wall layers, but no perivascular tissue damage (black arrows). Isolated intimal carbonization on the opposite side (black arrowhead). *C* artifact caused by the OCT catheter, *L* lumen. Bar=1 mm

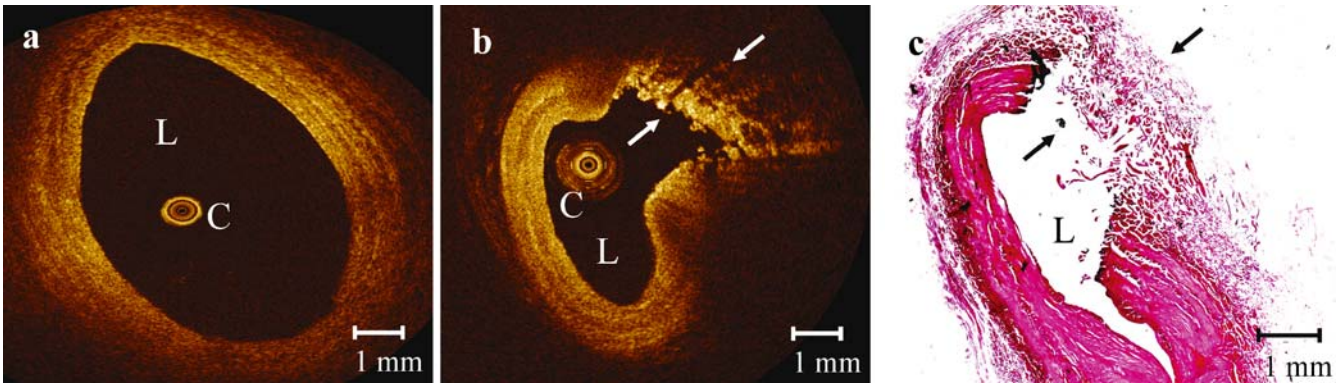


Fig. 5a–c Subcutaneous bovine leg vein before and after ELT with high energy density (35 J/cm). **a** OCT image before ELT reveals normal three-layered appearance of the vessel wall with normal lumen width. **b** OCT image immediately after ELT treatment demonstrates a severe thermal lesion with carbonization and

transmurular vessel wall disruption with preserved vein structure of the contralateral wall segment. **c** Histological cross section (hematoxylin/eosin staining; magnification 40×) with transmurular destruction of the vascular wall and surrounding perivascular tissue. *C* artifact caused by the OCT catheter, *L* lumen. Bar=1 mm

failure of thermal endovascular therapy of varicose veins, such that subsequent therapy could be more easily guided to the best spot.

Limitations

Our study has several limitations. First, we used venous segments derived from amputated bovine limbs. The absence of perfusion could result in changes to vessel wall structure. However, the effect of post-mortem tissue changes over a period of 3 h (the maximum time between death and OCT imaging in the present study) on venous optical properties should be minimal. Second, we studied thermal effects on veins of young healthy cows. An extrapolation of the observed tissue alterations cannot unreservedly be applied to dilated insufficient human veins. One important limitation of OCT for use in vivo relates to the inability to directly penetrate blood using the currently used infrared signal. Due to differences in refraction between erythrocytes and blood plasma, the examination must be conducted in the absence of blood. In order to fulfil this requirement, a special, double-lumen low-pressure balloon catheter has been developed that permits temporary proximal occlusion of the vessel [32]. At the same time, the vascular lumen is irrigated with physiological normal saline or Ringer's lactate solution. Several studies of patients with coronary heart disease have confirmed the feasibility of OCT in principle [36–38]. Due to the minimal residual blood flow following endovenous therapy and the significant narrowing of the venous lumen,

it can be postulated that simple irrigation with 10–20 ml of normal saline will be sufficient to facilitate adequate image quality. Placement of the OCT probe in highly atherosclerotic and severely narrowed arteries implies that passage of the therapeutically obliterated venous lumen with the 0.4-mm OCT probe should be accomplished without difficulty [8, 38, 39].

Conclusion

The present study demonstrates that endoluminal OCT is capable of visualizing the structure of normal venous wall with a resolution comparable to that of histology. In addition, OCT visualized different degrees of thermal changes of the vascular wall following endoluminal radiofrequency ablation or laser therapy. The ability of OCT to accurately characterize vessel wall alterations ex vivo suggests that this new technique may hold promise for a better understanding of the thermal effects that occur during endoluminal venous therapy in vivo. Information on thermal alterations might lead to more sophisticated and adapted treatment options for endoluminal varicose vein treatment in the future.

Acknowledgements We thank our research staff at the Ludwig Maximilians University of Munich. A substantial part of the data of this study originated from the doctoral theses of cand. med. Kathrin Hunger. The study was partially funded by the Friedrich-Bauer-Stiftung. Dr. Meissner served as a consultant for Siemens AG, Medical Solutions, during the time this study was conducted.

References

- Brezinski ME, Tearney GJ, Bouma B, Boppart SA, Pitris C, Southern JF, Fujimoto JG (1998) Optical biopsy with optical coherence tomography. *Ann N Y Acad Sci* 838:68–74
- Brezinski ME, Tearney GJ, Bouma BE, Boppart SA, Hee MR, Swanson EA, Southern JF, Fujimoto JG (1996) Imaging of coronary artery microstructure (in vitro) with optical coherence tomography. *Am J Cardiol* 77:92–93
- Fujimoto JG, Boppart SA, Tearney GJ, Bouma BE, Pitris C, Brezinski ME (1999) High resolution in vivo intrarterial imaging with optical coherence tomography. *Heart* 82:128–133
- Kume T, Akasaka T, Kawamoto T, Watanabe N, Toyota E, Neishi Y, Sukmawan R, Sadahira Y, Yoshida K (2005) Assessment of coronary intima-media thickness by optical coherence tomography: comparison with intravascular ultrasound. *Circ J* 69:903–907
- Brezinski M (2002) Characterizing arterial plaque with optical coherence tomography. *Curr Opin Cardiol* 17:648–655
- Patwari P, Weissman NJ, Boppart SA, Jesser C, Stamper D, Fujimoto JG, Brezinski ME (2000) Assessment of coronary plaque with optical coherence tomography and high-frequency ultrasound. *Am J Cardiol* 85:641–644
- Yabushita H, Bouma BE, Houser SL, Aretz HT, Jang IK, Schlendorf KH, Kauffman CR, Shishkov M, Kang DH, Halpern EF, Tearney GJ (2002) Characterization of human atherosclerosis by optical coherence tomography. *Circulation* 106:1640–1645
- Meissner OA, Rieber J, Babaryka G, Oswald M, Reim S, Siebert U, Redel T, Eibel R, Mueller-Lisse U, Reiser M, Mueller-Lisse UG (2006) [Intravascular optical coherence tomography: differentiation of atherosclerotic plaques and quantification of vessel dimensions in crural arterial specimens]. *Rofo* 178:214–220
- Feied C, Min RJ, Weiss R, Zimmet SE, Hashemiyoon R (2005) Varicose vein treatment with endovenous laser therapy. <http://www.emedicine.com/derm/topic750.htm>
- Merchant RF, Pichot O (2005) Long-term outcomes of endovenous radiofrequency obliteration of saphenous reflux as a treatment for superficial venous insufficiency. *J Vasc Surg* 42:502–509; discussion 509
- Proebstle TM, Moehler T, Gul D, Herdemann S (2005) Endovenous treatment of the great saphenous vein using a 1,320 nm Nd:YAG laser causes fewer side effects than using a 940 nm diode laser. *Dermatol Surg* 31:1678–1683; discussion 1683–1684
- Goldman MP (2000) Closure of the greater saphenous vein with endoluminal radiofrequency thermal heating of the vein wall in combination with ambulatory phlebectomy: preliminary 6-month follow-up. *Dermatol Surg* 26:452–456
- Kabnick LS (2006) Outcome of different endovenous laser wavelengths for great saphenous vein ablation. *J Vasc Surg* 43:88–93
- Proebstle TM, Lehr HA, Kargl A, Espinola-Klein C, Rother W, Bethge S, Knop J (2002) Endovenous treatment of the greater saphenous vein with a 940-nm diode laser: thrombotic occlusion after endoluminal thermal damage by laser-generated steam bubbles. *J Vasc Surg* 35:729–736
- Lurie F, Creton D, Eklof B, Kabnick LS, Kistner RL, Pichot O, Schuller-Petrovic S, Sessa C (2003) Prospective randomized study of endovenous radiofrequency obliteration (closure procedure) versus ligation and stripping in a selected patient population (EVOLVEs Study). *J Vasc Surg* 38:207–214
- Lurie F, Creton D, Eklof B, Kabnick LS, Kistner RL, Pichot O, Sessa C, Schuller-Petrovic S (2005) Prospective randomised study of endovenous radiofrequency obliteration (closure) versus ligation and vein stripping (EVOLVEs): two-year follow-up. *Eur J Vasc Endovasc Surg* 29:67–73
- Merchant RF, Pichot O, Myers KA (2005) Four-year follow-up on endovascular radiofrequency obliteration of great saphenous reflux. *Dermatol Surg* 31:129–134
- Perkowski P, Ravi R, Gowda RC, Olsen D, Ramaiah V, Rodriguez-Lopez JA, Diethrich EB (2004) Endovenous laser ablation of the saphenous vein for treatment of venous insufficiency and varicose veins: early results from a large single-center experience. *J Endovasc Ther* 11:132–138
- Rautio T, Ohinmaa A, Perala J, Ohtonen P, Heikkinen T, Wiik H, Karjalainen P, Haukipuro K, Juvonen T (2002) Endovenous obliteration versus conventional stripping operation in the treatment of primary varicose veins: a randomized controlled trial with comparison of the costs. *J Vasc Surg* 35:958–965
- Mundy L, Merlin TL, Fitridge RA, Hiller JE (2005) Systematic review of endovenous laser treatment for varicose veins. *Br J Surg* 92:1189–1194
- Schmedt CG, Sroka R, Steckmeier S, Meissner OM, Babaryka G, Hunger K, Ruppert V, Sadeghi-Azandaryani M, Steckmeier BM (2006) Investigation on radiofrequency and laser (980 nm) effects after endoluminal treatment of saphenous vein insufficiency in an ex vivo model. *Eur J Vasc Endovasc Surg* 32:318–325
- Fujimoto JG (2003) Optical coherence tomography for ultrahigh resolution in vivo imaging. *Nat Biotechnol* 21:1361–1367
- Fujimoto JG, Brezinski ME, Tearney GJ, Boppart SA, Bouma B, Hee MR, Southern JF, Swanson EA (1995) Optical biopsy and imaging using optical coherence tomography. *Nat Med* 1:970–972
- Huang D, Li Y, Radhakrishnan S (2004) Optical coherence tomography of the anterior segment of the eye. *Ophthalmol Clin North Am* 17:1–6
- Min RJ, Zimmet SE, Isaacs MN, Forrestal MD (2001) Endovenous laser treatment of the incompetent greater saphenous vein. *J Vasc Interv Radiol* 12:1167–1171
- Navarro L, Min RJ, Bone C (2001) Endovenous laser: a new minimally invasive method of treatment for varicose veins—preliminary observations using an 810 nm diode laser. *Dermatol Surg* 27:117–122
- Weiss RA, Weiss MA (2002) Controlled radiofrequency endovenous occlusion using a unique radiofrequency catheter under duplex guidance to eliminate saphenous varicose vein reflux: a 2-year follow-up. *Dermatol Surg* 28:38–42
- Min RJ, Khilnani N, Zimmet SE (2003) Endovenous laser treatment of saphenous vein reflux: long-term results. *J Vasc Interv Radiol* 14:991–996
- Huang Y, Jiang M, Li W, Lu X, Huang X, Lu M (2005) Endovenous laser treatment combined with a surgical strategy for treatment of venous insufficiency in lower extremity: a report of 208 cases. *J Vasc Surg* 42:494–501; discussion 501
- Proebstle TM, Krummenauer F, Gul D, Knop J (2004) Nonocclusion and early reopening of the great saphenous vein after endovenous laser treatment is fluence dependent. *Dermatol Surg* 30:174–178

31. Landis JR, Koch GG (1977) The measurement of observer agreement for categorical data. *Biometrics* 33:159–174
32. Regar E, Schaar JA, Mont E, Virmani R, Serruys PW (2003) Optical coherence tomography. *Cardiovasc Radiat Med* 4:198–204
33. Meissner OA, Rieber J, Babaryka G, Oswald M, Reim S, Siebert U, Redel T, Reiser M, Mueller-Lisse U (2006) Intravascular optical coherence tomography: comparison with histopathology in atherosclerotic peripheral artery specimens. *J Vasc Interv Radiol* 17:343–349
34. Corcos L, Dini S, De Anna D, Marangoni O, Ferlino E, Procacci T, Spina T, Dini M (2005) The immediate effects of endovenous diode 808-nm laser in the greater saphenous vein: morphologic study and clinical implications. *J Vasc Surg* 41:1018–1024; discussion 1025
35. Timperman PE, Sichlau M, Ryu RK (2004) Greater energy delivery improves treatment success of endovenous laser treatment of incompetent saphenous veins. *J Vasc Interv Radiol* 15:1061–1063
36. Jang IK, Bouma BE, Kang DH, Park SJ, Park SW, Seung KB, Choi KB, Shishkov M, Schlendorf K, Pomerantsev E, Houser SL, Aretz HT, Tearney GJ (2002) Visualization of coronary atherosclerotic plaques in patients using optical coherence tomography: comparison with intravascular ultrasound. *J Am Coll Cardiol* 39:604–609
37. Jang IK, Tearney G, Bouma B (2001) Visualization of tissue prolapse between coronary stent struts by optical coherence tomography: comparison with intravascular ultrasound. *Circulation* 104:2754
38. Jang IK, Tearney GJ, MacNeill B, Takano M, Moselewski F, Iftima N, Shishkov M, Houser S, Aretz HT, Halpern EF, Bouma BE (2005) In vivo characterization of coronary atherosclerotic plaque by use of optical coherence tomography. *Circulation* 111:1551–1555
39. Rieber J, Meissner O, Babaryka G, Reim S, Oswald M, Koenig A, Schiele TM, Shapiro M, Theisen K, Reiser MF, Klauss V, Hoffmann U (2006) Diagnostic accuracy of optical coherence tomography and intravascular ultrasound for the detection and characterization of atherosclerotic plaque composition in ex-vivo coronary specimens: a comparison with histology. *Coron Artery Dis* 17:425–430